Materials Science inc. Nanomaterials & Polymers

Mesoporous Si-MCM-41/Polymer as a pH-Responsive Drug Delivery System for Cancer Therapy

Mina Maghsoudi,[a] Mojtaba Abbasian,*[a] Khalil Farhadi,[b] Farideh Mahmoodzadeh,*[c] Marjan Ghorbani,[d] and Mehdi Hoseinzadeh[e]

Nano-controlled drug delivery systems such as polymer nanocomposites introduce new strategies for the cancer prevention, diagnosis and treatment. In this study, we designed a biocompatible polymer Nanocomposites (NCs) based on modified mobil composition of matter No. **41** (MCM-41) nanoparticles (MCM-41-NH_2) and copolymer grafted chitosan by acrylamide and acrylic acid (CS-graft-poly (AAm-co-AA) as a pH-sensitive polymer, and employed for targeted anticancer drug delivery. Doxorubicin (DOX) is a potent drug for cancer therapy. DOX was loaded into the synthesized polymer NCs MCM-41-NH_2-CS-graft-poly (AAm-co-AA) by formation electrostatic attraction between the positive charge of the DOX and the anionic charge of the poly acrylic acid (PAA), and poly acrylamide (PAAm). Free DOX diffuse rapidly into nucleus, and kill cancerous cells by interaction with deoxyribonucleic acid (DNA). But, keeping active of free anticancer drugs after reaching at the nucleus is difficult due to the bio barriers. Using DOX-loaded into the mentioned polymer NCs can be decreased the toxicity effects (side effects) of DOX on the normal cells and enhance its efficiency on the tumorous cells The release of DOX from the MCM-41-NH_2-CS-g-poly (AAm-co-AA) was studied at acidic conditions (on the human breast epithelial adenocarcinoma (MCF-7) cancer cells, pH 5.3 and 40 °C). The cytotoxicity of the DOX loaded into MCM-41-NH_2-CS-g-poly (AAm-co-AA) on the (MCF-7) cancer cells was evaluated by using MTT (3-(4,5-Dimethylthiazol-2-yl)-2,5-diphenyltetrazolium bromidefor). The results show that synthetic mesoporous Si-MCM-41/ polymer can act as a targeted drug delivery system for the treatment of MCF-7 cancerous cell.

1. Introduction

The cases and deaths from cancer are high in the world. Getting cancerous tissue to high drug concentration without adverse effects on the healthy tissue is the most important issue in cancer therapy. Nano-controlled drug delivery systems introduce new strategies for the cancer prevention, diagnosis and treatment.[1]

The drug delivery system demands intravenous administration. Therefore, ensuring high safety, and no adverse effects on healthy cells of the body is essential for the drug delivery systems.[2] The mesoporous silica nanoparticles (MSNs) have received much attention in drug delivery due to the features such as biocompatibility, the high specific surface area, tunable pore size, physicochemical stability, easy surface modification by abundant silanol (Si-OH) groups in their surface, hexagonal structure, a long blood circulation time, selective accumulation in cancerous cells by enhanced permeability and retention (EPR) effect.[2,3] The targeted drug delivery systems such as nanocomposite have been employed for decreasing the toxic side effects, and enhancing anticancer efficiency. The targeted for the example pH-responsive is dependent to the type of polymer. Polymer nanocomposite (NCs) can be synthesized by adding nanofillers such as nanosilica MCM-41 to the polymer matrix. Using modified mesoporous with smart polymers[4–6] can be delivered drug to targeted tissue or cell at a specified time and site with controlled release speed. The loading capacity of the drug can also be increased. Chitosan (CS) is a natural biopolymer. Due to its primary amine and hydroxyl groups, biocompatibility,[2] nontoxicity and antibacterial properties is mainly utilized in nanocarriers, pharmaceutical applications, cancer targeted therapy[7] and tissue engineering.[8,9] The amino groups of chitosan have a pKa value of 6.5 and makes it as pH sensitive polymer (smart polymer). The cancer cells differ from the normal cells due to biological features, more metabolism, more cell temperature, less intracellular pH and higher content of reducing enzymes. In stimuli-responsive[10] drug delivery system (SRDDS), release drugs are controlled by environmental stimuli. These stimuluses are classified into internal and external agents. From internal factors can be referred to cancer cell pH,[2,11–17] enzymes,[18–20] temperature.[21,22]

[a] *Dr. M. Maghsoudi, Prof. M. Abbasian*
Department of Chemistry, Payame Noor University, P.O. BOX: 19395–3697, Tehran, Iran
E-mail: m_abbasian20@yahoo.com
m_abbasian@pnu.ac.ir
[b] *Prof. K. Farhadi*
Department of Analytical Chemistry, Urmia University, Urmia, Iran
[c] *Dr. F. Mahmoodzadeh*
Halal Research Center of IRI, FDA, Tehran, Iran
E-mail: mahmoodzadeh.farideh@gmail.com
mahmoudzadeh.f@arasfz.ir
[d] *Dr. M. Ghorbani*
Stem Cell Research Center, Tabriz University of Medical Sciences, Tabriz, Iran
[e] *Dr. M. Hoseinzadeh*
Marand Faculty of Technical and Engineering, University of Tabriz, Tabriz, Iran

Supporting information for this article is available on the WWW under https://doi.org/10.1002/slct.202002071

The external factors are such magnetic field[23] and radiation of light.[24]

Excited cancerous tissue has pH 5.4, and have acidic conditions in comparing to the normal tissue pH (7.4). For this reason, using the modified mesoporous silica nanoparticles (MSNs) with smart polymer can be the effective therapeutic strategy. The physical, chemical and biological features of the chitosan can be improved with materials such as acrylic acid (AA), acrylamide (AAm). The poly acrylic acid (PAA) is a biocompatible anionic polymer, and the poly acrylamide (PAAm) extensively utilized in drug delivery and biomedical application. MCM-41 type mesoporous silica nanoparticles (MSNs) and the poly acrylic acid (PAA) are approved by food and drug Administration (FDA).[1,9]

Doxorubicin (DOX) is a potent drug for cancer therapy. DOX is a cationic drug[7] (Doxorubicin pKa = 8.3) and contain positively charged in physiological condition due to the functional amine groups,[25] and can be simply loaded into mesoporous Si-MCM-41/smart polymer by formation electrostatic attraction between the positive charge of the DOX and the anionic charge of the smart polymer.

In this project, we fabricated a polymer NCs based on modified MCM-41 and pH-sensitive polymer for targeted anticancer therapy. Mesoporous Si-MCM-41 was synthesized using Sol-gel method. The modified MCM-41 nanoparticles (MCM-41-NH_2) was synthesized using (3-APTES) as modifier on the surface of MCM-41. The (MCM-41-NH_2) nanoparticles made chemical interaction with biopolymer chitosan. In the presence of KPS as initiator formed active radicals on the modified MCM-41-chitosan and in-situ polymerization performed by adding the acrylamide (AAm), and acrylic acid (AA) as monomers. Initiator of KPS is very appropriate for the aqueous solution. In the in-situ polymerization technique (MCM-41-NH_2) nanoparticles spread into the polymer matrix homogenously. Polymer NCs as MCM-41-NH_2-CS-g-poly (AAm-co-AA) was characterized using Fourier transform infrared spectroscopy (FT-IR), scanning electron microscope (FE-SEM), Energy dispersive spectrum (EDS) analysis, X-ray powder diffraction (XRD). The thermal properties were measured by using thermo-gravimetric analysis (TGA). the specific surface area (ap), pore volume (Vp), and the pore diameters (rp) was measured for the MCM-41, functionalized MCM-41 (MCM-41-NH_2), and MCM-41-NH_2-CS-g-poly (AAm-co-AA) by Brunauer-Emmett-Teller (BET) and Barrett-Joyner Halenda (BJH) analysis. Doxorubicin (DOX) is a potent drug for cancer therapy, and have fluorescent properties. DOX loaded into MCM-41-NH_2-CS-g-poly (AAm-co-AA). The release of pH-responsive DOX from MCM-41-NH_2-CS-g-poly (AAm-co-AA) was studied. The cytotoxicity assay measured by MTT of MCM-41-NH_2-CS-g-poly (AAm-co-AA)-DOX (as DOX-nanocarrier), and on the human breast epithelial adenocarcinoma (MCF-7) cells. To investigate the morphological features in the nucleus of an apoptosis cell used DAPI staining. Treated MCF7 cells with DOX-loaded MCM-41-NH_2-CS-g-poly (AAm-co-AA) nanocomposite (DOX-nanocarrier) revealed higher content of apoptotic cell nucleus morphology (chromatin density and fragmentation) than free DOX.

2. Results and Discussion

In this study, mesoporous silica nanoparticles (MSNs) used in drug delivery application due to unique properties such as specific surface area and large hole size. As showed in scheme 1 and 2, MCM-41-NH_2 was modified with chitosan (CS), grafting a co-polymer poly (AAm-co-AA) on their surface by in situ polymerization.

Doxorubicin (DOX) as anticancer drug encapsulated into the obtained MCM-41-NH_2-CS-g-poly (AAm-co-AA) by formation electrostatic attraction between the positive charge of the DOX and the the anionic charge of the polymer. The release of

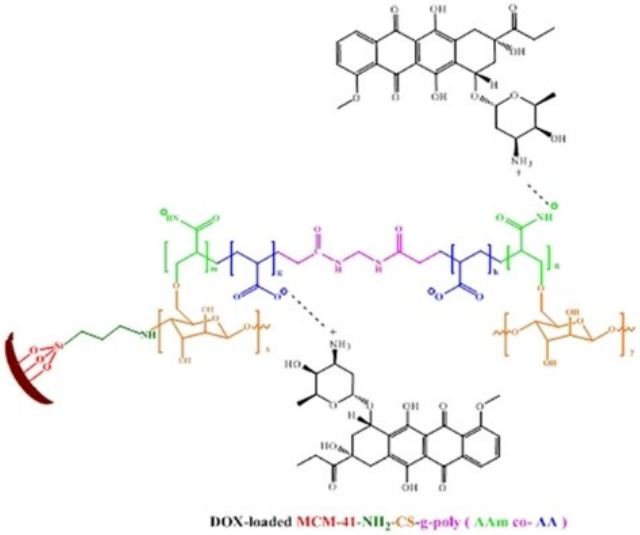

Scheme 1. The advanced strategy for the synthesis of [(MCM-41-NH2-CS-g-poly (AAm-co-AA)] nanocomposite.

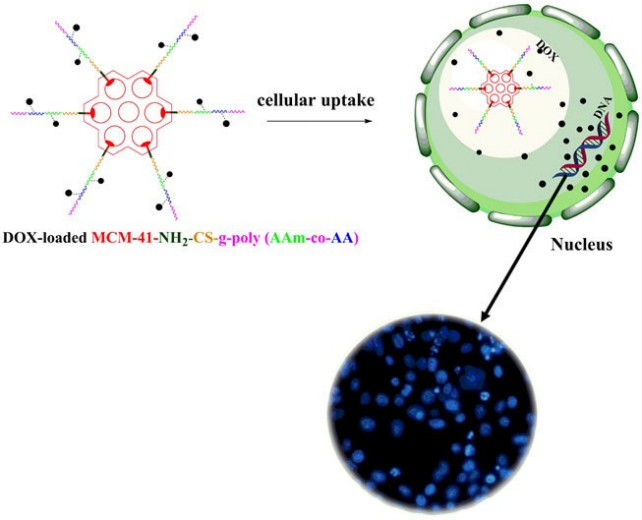

Scheme 2. Schematic structure for cellular uptake mechanism of doxorubicin (DOX) -loaded MCM-41-NH_2-CS-g-poly (AAm-co-AA) nanocomposite into cancerous cells.

the DOX from MCM-41-NH_2-CS-g-poly (AAm-co-AA) is as the smart pH-responsive process in cancerous cells.

DOX-loaded MCM-41-NH_2-CS-g-poly (AAm-co-AA) entered (MCF-7) cancer cells and interacted with DNA inside the nuclei. Treated MCF7 cells with DOX-loaded MCM-41-NH_2-CS-g-poly (AAm-co-AA) revealed high content of apoptotic cell nucleus morphology (chromatin density and fragmentation).

3. FTIR spectroscopy

The FT-IR spectra of MCM-41, amine-modified MCM-41, MCM-41-NH_2-CS-g-poly (AAm-co-AA) nanocomposite displays in Figure 1.

The FT-IR spectra of MCM-41 demonstrates the broad band of the silanol groups (Si-OH) at 3423 cm^{-1}, the asymmetric stretching vibration of the Si-O–Si at 1078 cm^{-1}, the symmetric stretching vibration of the Si-O–Si at 941 and 804 cm^{-1}, the bending vibration of the Si-O–Si at 459 cm^{-1}.

The FT-IR spectra of the amine-modified MCM-41 (MCM-41-NH_2) show new peaks in liken to pure MCM-41 such as the asymmetric and symmetric stretching vibrations of the methylene groups (CH_2) at 2931 and 2867 cm^{-1} respectively, the symmetric bending vibration of the amine groups (-NH_2) at 1635 cm^{-1}, the stretching vibration of the (C–N) at 1407 cm^{-1}, confirming that the modification of MCM-41 using (3-amino propyl) triethoxy silane (3-APTES) are performed successfully. The amine-modified MCM-41 (MCM-41-NH_2) enhance interaction with organic/polymeric combinations.[11]

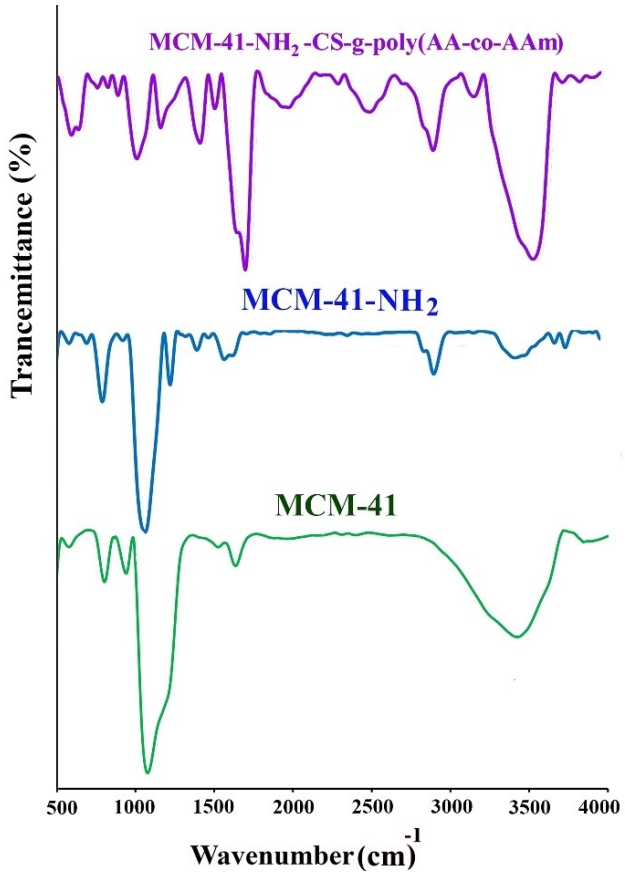

Figure 1. FT-IR spectra of MCM-41, MCM-41-NH_2, MCM-41-NH_2-CS-g-poly (AAm-co-AA) nanocomposite.

The FT-IR spectra of the synthetic MCM-41-NH_2-CS-g-poly (AAm-co-AA) nanocomposite exhibits the stretching vibration of the (O–H), and (N–H) groups at 3568 cm^{-1}, the stretching vibration of the aliphatic (C–H) at 2927 cm^{-1}, the asymmetric stretching vibration of the carbonyl (–COOH) group at 1728 cm^{-1}, the asymmetric stretching vibration of the carbonyl (CO-NH) at 1674 cm^{-1}, the symmetric stretching vibration of the carbonyl (–COO) group at 1438 cm^{-1} and the asymmetric stretching vibration of the Si–O–Si at 1033 cm^{-1}.

3.1. X-ray powder diffraction (XRD) patterns

The low-angle X-ray diffraction (LXRD), and XRD patterns of MCM-41, amine-modified MCM-41 (MCM-41-NH_2), Chitosan (CS), and MCM-41-NH_2-CS-g-poly (AAm-co-AA) nanocomposite (NCs) are displayed in Figure 2.

The low-angle X-ray diffraction (LXRD) pattern of the mesoporous silica MCM-41 (Figure 2a) show three peaks at $2\theta = 2.7°$ (strong and sharp), $2\theta = 4.2°$ and 4.8° (weak with low intensity) corresponding to well-ordered hexagonal structure of the mesoporous silica (MCM-41).

The (LXRD) pattern of the amine-modified MCM-41 (MCM-41-NH2) exhibit peaks at $2\theta = 1.1°$, $2\theta = 2.1$, and 2.6°. Because of modification MCM-41 with (3-amino propyl) triethoxy silane (3-APTES), the peak intensity is decreased and the peak region is shifted in compairing with pure MCM-41 (Figure 2b).

A strong and sharp peak in the XRD pattern of chitosan (CS) (Figure 2c) is observed at 20.1° that indicate crystallinity and making of the hydrogen bonds among (-OH), (-NH2), and (CH3-CONH) functional groups.[9]

The XRD diagram of the MCM-41-NH_2-CS-g-poly (AAm-co-AA) nanocomposite (Figure 2d) shows that, the peak intensity is reduced after polymerization and the presence nanoparticles (MCM-41-NH_2) at 5–15° and 15–30° in liken to pure chitosan (CS).

3.2. Thermo-gravimetric (TGA) analysis

The TGA curves of MCM-41, amine-modified MCM-41 (MCM-41-NH_2), MCM-41-NH_2-CS-g-poly (AAm-co-AA) nanocomposite are displayed in Figure 3.

The TGA curves of MCM-41 exhibit three separate thermal degradation steps: (30-180 °C), (180-500 °C), and (500-800 °C). The thermal degradation at (30-180 °C) is corresponded to loss of water/organic solvents adsorbed on the surface (–OH) groups, and into the pores. The mass loss at (180–500 °C) is owing to degradation of covalently bonded organics. The thermal decomposition of functional (Si-OH) groups occurs at (500-800 °C).[26,27]

The TGA curve of amine-modified MCM-41 (MCM-41-NH_2) display water and organic solvent loss at (30 to 150 °C). The thermal decomposition of (3-amino propyl) triethoxy silane (3-APTES) as modifier occurs between 150 and 800 °C.

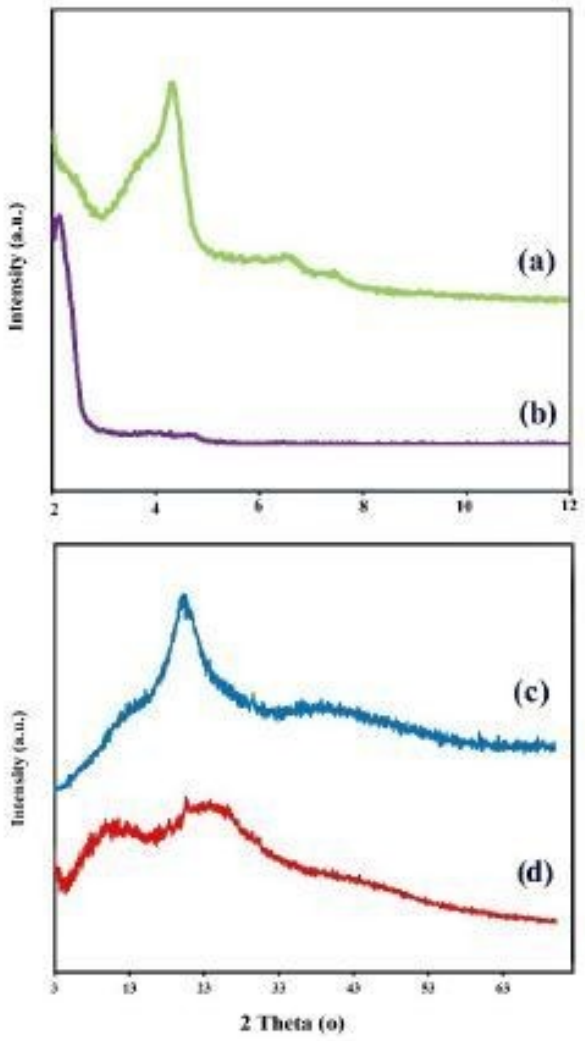

Figure 2. XRD patterns of (a) MCM-41, (b) MCM-41-NH_2, (c) Chitosan (CS), (d) MCM-41-NH_2-CS-g-poly (AAm-co-AA) nanocomposite (NCs).

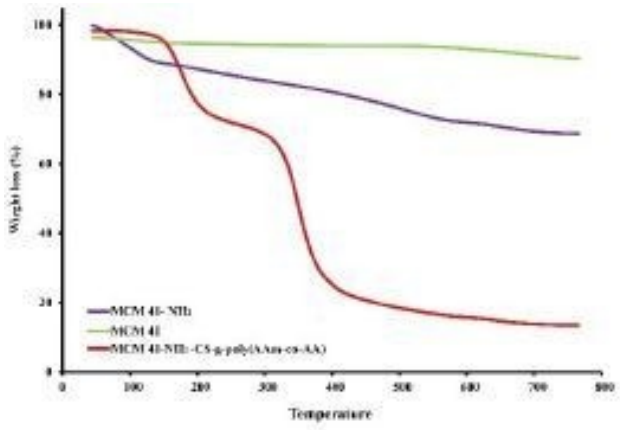

Figure 3. TGA thermograms of MCM-41, MCM-41-NH_2, MCM-41-NH_2-CS-g-poly (AAm-co-AA) nanocomposite.

The TGA thermogram of the MCM-41-NH_2-CS-graft-poly-(AAm-co-AA) nanocomposite exhibit four separate mass loss steps: the initial step (below 140 °C) is related to evaporation of water. The second step (140–300 °C) is associated to loss of NH_2 of amide side groups in poly acrylamide (PAAm) and N, N′-methylene bis acrylamide (MBA) as cross-linker, and release CO_2 from the functional group of poly acrylic acid (PAA). The third step (300 to 600 °C) is corresponding to breakdown components of polymeric chain. In the final step, the degradation of the silanol (Si-OH) groups occur between 600 and 800 °C.

3.3. Scanning electron microscopy (SEM) images

The surface morphology for the MCM-41, amine-modified MCM-41 (MCM-41-NH_2), MCM-41-NH_2-CS-g-poly (AAm-co-AA) nanocomposite are investigated in Figure 4.

As can be observed in (Figure 4a), the mesoporous Si-MCM-41 exhibit smooth, spherical, and orderly morphology. The particles have nanometer size in about 29 nm. The SEM image of the amine-modified MCM-41 (MCM-41-NH_2) are shown in (Figure 4b). The particles become smoother, and larger after the modification mesoporous Si- MCM-41 with (3-amino propyl) triethoxy silane (3-APTES). The particles have the spherical morphology, and nanometer size in about 56 nm.[1,11]

The FE-SEM image of the MCM-41-NH_2-CS-graft-poly-(AAm-co-AA) nanocomposite are shown in (Figure 4d). The FE-SEM image exhibit the growth of PAAm, and PAA onto chitosan (CS) surface. The polymeric network has tight surface due to cross-linker MBA.

3.4. Energy dispersive spectrum (EDS) analysis

As observed in table 1, the energy dispersive spectrum (EDS) of MCM-41-NH_2-CS-graft-poly-(AAm-co-AA) nanocomposite revealed the existence of C (60.8 %), O (38 %), N (0.4 %), Si (0.4 %), and K (0.4 %) elements.

3.5. Brunauer-Emmett-Teller (BET) and Barrett-Joyner Halenda (BJH) study

The nitrogen adsorption/desorption isotherms are performed in order to examine pore size of mesoporous materials (in Figure 5).

The mesopore channels in MCM-41 type mesoporous silica nanoparticles (MSNs) are confirmed by specific type IV nitrogen adsorption/desorption isotherms. The results show that the specific surface area (ap), pore volume (Vp), and the pore diameters (rp) are about (665.66) m^2g^{-1}, (0.7) cm^3g^{-1} and (1.26) nm respectively for the MCM-41 (Table 2).

For amine-modified MCM-41, the N_2 adsorption/desorption isotherm reveals an significant decrease in surface area (81.140) m^2g^{-1}, pore volume (0.31) cm^3g^{-1} and an increase in the wall diameter value about (12.52) nm due to grafting of (3-amino propyl) triethoxy silan (3-APTES) onto the surface of MCM-41.

In the N_2 adsorption/desorption isotherm for the obtained MCM-41-NH_2-CS-g-poly (AAm-co-AA) nanocomposite, a de-

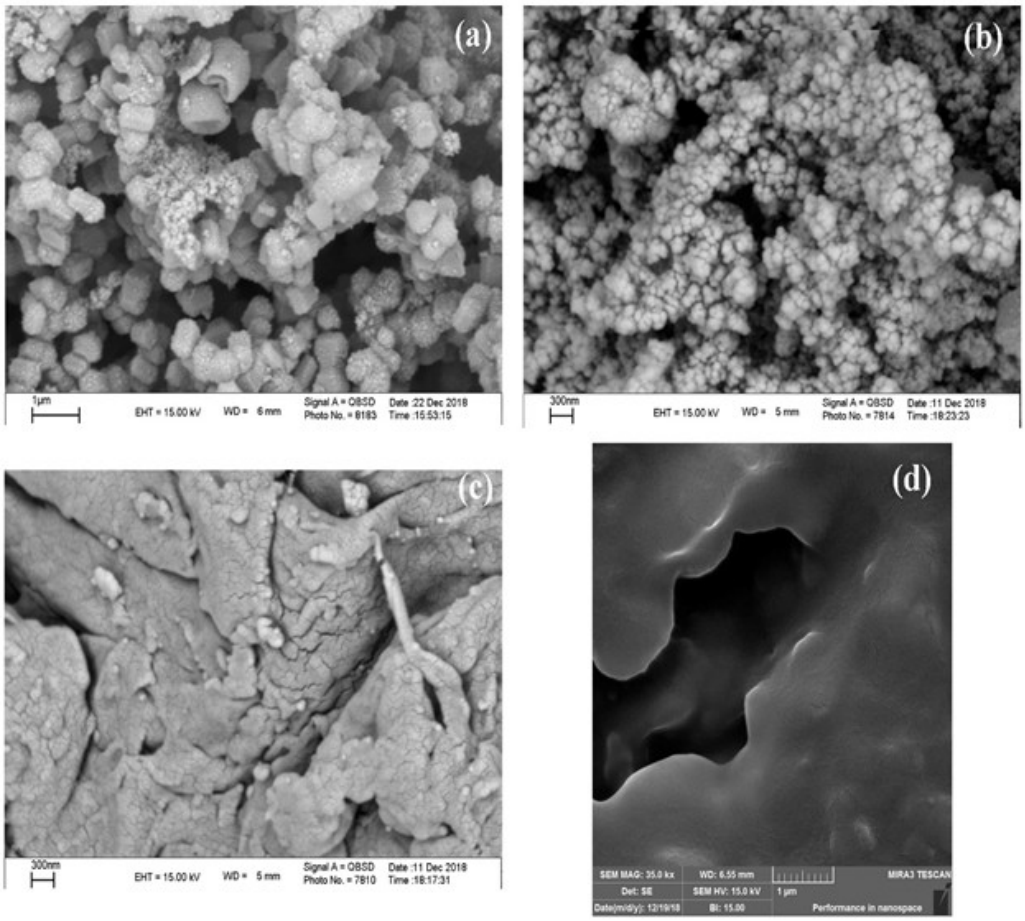

Figure 4. FE-SEM images of (a) MCM-41 (scale bars: 1 micro meter), (b) MCM-41-NH_2 (scale bars:300 nano meter), (c) Chitosan (CS) (scale bars: 300 nano meter), (d) MCM-41-NH_2-CS-g-poly (AAm-co-AA) nanocomposite(scale bars: 1 micro meter).

Table 1. The energy dispersive spectrum (EDS) of MCM-41-NH_2-CS-graft-poly-(AAm-co-AA) nanocomposite.

Element	Line Type	Apparent Concentration	k Ratio	Wt%	Wt% Sigma	Atomic %	Standard Label	Factory Standard	Standard Calibration Date
C	K series	39.54	0.39535	60.82	0.58	67.59	C Vit	Yes	
N	K series	0.30	0.00053	0.43	0.87	0.41	BN	Yes	
O	K series	28.65	0.09639	37.98	0.40	31.69	SiO2	Yes	
Si	K series	0.35	0.00276	0.38	0.03	0.18	SiO2	Yes	
K	K series	0.31	0.00266	0.35	0.04	0.12	KBr	Yes	
Ca	K series	0.04	0.00032	0.04	0.04	0.01	Wollastonite	Yes	
Total:				100.00		100.00			

Table 2. Textural parameters from nitrogen sorption isotherms

Sample	a_p (m^2/g)	V_p (cm^3/g)	$r_{p,peak}$ (nm)
MCM-41	665.66	0.7	1.26
MCM-41-NH_2	81.140	0.31	12.52
MCM-41-NH_2-CS-g-poly (AAm-co-AA) nanocomposite	−2.0022E-01	2.3356E-02	16.66

crease in surface area, pore volume, and an increase in the wall diameter were also observed owing to grafting of MCM-41-NH_2 with polymeric chain.

3.6. Studying in vitro DOX release from MCM-41-NH_2-CS-g-poly (AAm-co-AA) nanocomposite

The biodissemination and pharmacokinetics of DOX were advanced via the MCM-41-NH_2-CS-g-poly (AAm-co-AA) nanocomposite improved as a nanocarrier for drug delivery systems. The synthesized nano carrier contained various functional groups –COOH, –$CONH_2$, OH and NH_2. Achieving the controlled release of drugs is the chief purpose of these nanocarrier. The cancer cells differ from the normal cells due to biological features, more metabolism, more cell temperature, less intra-

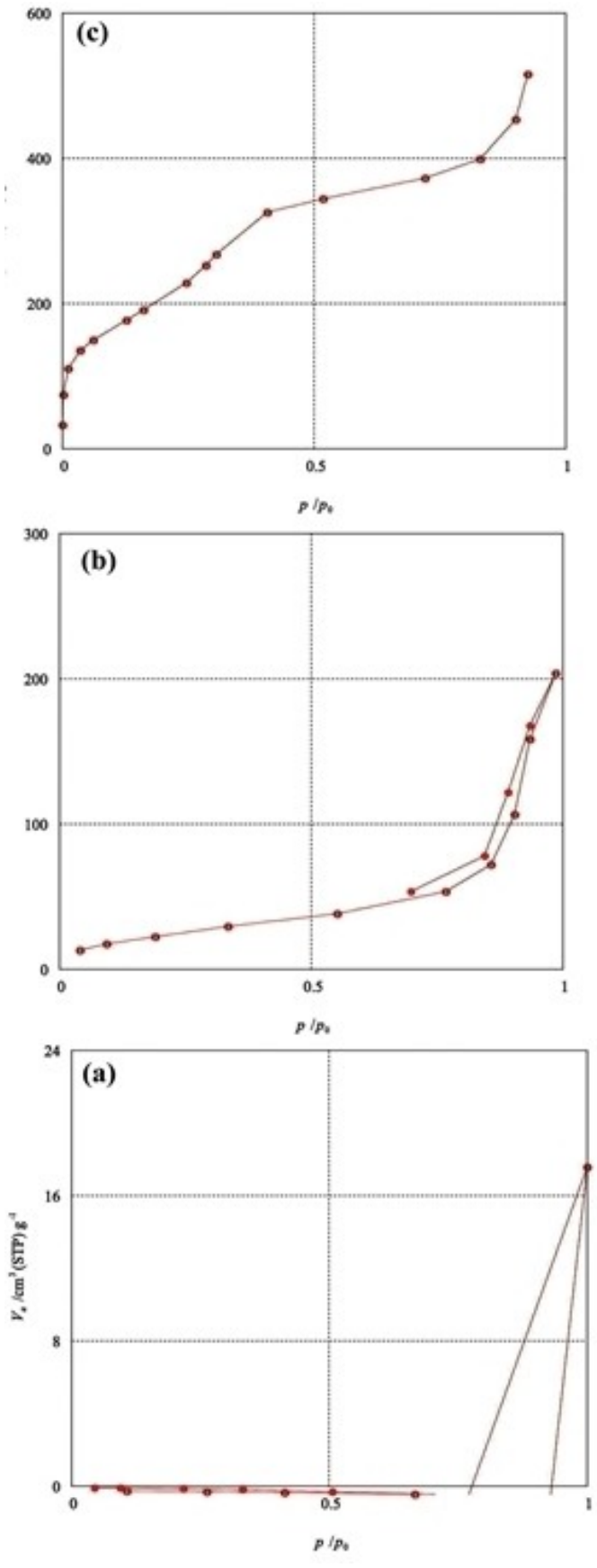

Figure 5. The N_2 adsorption and desorption isotherms of (a) MCM-41, (b) MCM-41-NH_2, (c) MCM-41-NH_2-CS-g-poly (AAm-co-AA) nanocomposite.

cellular pH and higher content of reducing enzymes. Hence, it can control content release of anticancer drugs by using temperature and pH responsive polymeric nanocarrier.

DOX is the appropriate model drug in order to load into the MCM-41-NH_2-CS-g-poly (AAm-co-AA) nanocomposite for controlled drug delivery systems via the this cause: DOX is a cationic drug (Doxorubicin pKa = 8.3) and contain positively charged in physiological condition due to the functional amine groups and can be simply loaded into polymeric compound having negative charge on surface such as MCM-41-NH_2-CS-g-poly (AAm-co-AA) polymeric nanocomposite by formation electrostatic attraction (hydrogen bonds) between the anionic –COOH ($–COO^-$), $–CONH_2$ ($–CONH^-$), OH ($–O^-$) and NH_2 ($–NH^-$) groups with positive charge of DOX amino groups.

The release of DOX from MCM-41-NH_2-CS-g-poly (AAm-co-AA)-DOX was investigated using dialysis method at normal physiological condition (pHs = 7.4 and 37 °C) and at acidic conditions (excited cancerous tissue, pH 5.3 and 40 °C). The release speed of DOX was calculated according to the following equation:

$$R = M1/M0$$

Where M1 is the cumulative mass of DOX released from MCM-41-NH_2-CS-g-poly (AAm-co-AA)-DOX at a special time, and M0 is the total loading amount of DOX in the MCM-41-NH_2-CS-g-poly (AAm-co-AA) nanocomposite.

At neutral pH (7.4), the carboxyl, and amine groups of the MCM-41-NH_2-CS-g-poly (AAm-co-AA) nanocomposite de-protonated and caused to formation electrostatic attraction (hydrogen bonds) between anionic charges of MCM-41-NH_2-CS-g-poly (AAm-co-AA) nanocomposite containing: [carboxylate anion ($–COO^-$), anion ($–CONH^-$)] groups and the positive charge of DOX amino groups. As a result, slow drug release was observed. As shown in Figure 6 less than 8% of loaded DOX was released from MCM-41-NH_2-CS-g-poly (AAm-co-AA)- DOX

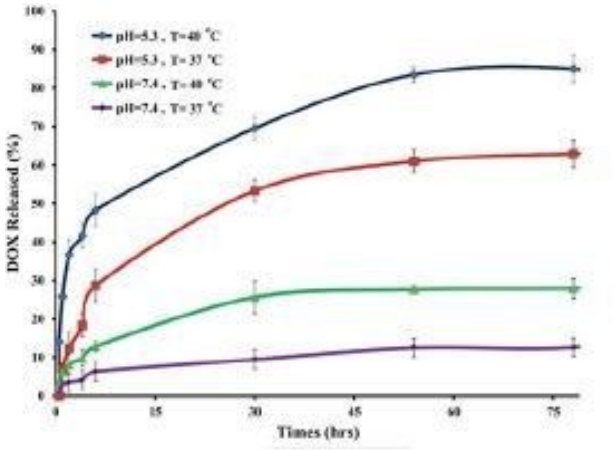

Figure 6. In vitro release profiles of MCM-41-NH_2-CS-g-poly (AAm-co-AA)-DOX under various pHs at (37 °C) and (40 °C).

after the continuous incubation at normal physiological condition (pHs = 7.4 and 37 °C) for 75 h.

At acidic conditions (excited cancerous tissue, pH 5.3 and 40 °C), the amine groups of DOX protonated and lead to fast release of DOX from MCM-41-NH_2-CS-g-poly (AAm-co-AA)-DOX. According to Figure 8, the drug release values in pH 5.3 and 40 °C were nearly 90% during 75 h, indicating that the release of DOX from MCM-41-NH_2-CS-g-poly (AAm-co-AA) nanocomposite is the temperature, and pH-responsive process.

3.7. In vitro cytotoxicity Study

3.7.1. MTT assay

The in-vitro cytotoxicity of MCM-41-NH_2-CS-g-poly (AAm-co-AA) nanocomposite (as nanocarrier), DOX-loaded MCM-41-NH_2-CS-g-poly (AAm-co-AA) (as DOX-nanocarrier), and free DOX (DOX) were evaluated by 3-(4,5-dimethylthiazol-2-yl)-2,5-diphenyltetrazolium bromide (MTT) assay. In vitro MTT assay was used for the measurement of the cytotoxicity effects of free DOX, MCM-41-NH_2-CS-g-poly (AAm-co-AA) nanocomposite (as nanocarrier) and DOX-loaded MCM-41-NH_2-CS-g-poly (AAm-co-AA) (as DOX-nanocarrier) against the MCF7 cell during 24 h (in Figure 7.a) and 48 h (Figure 7.b) incubation times with concentration 50 μg mL^{-1}.

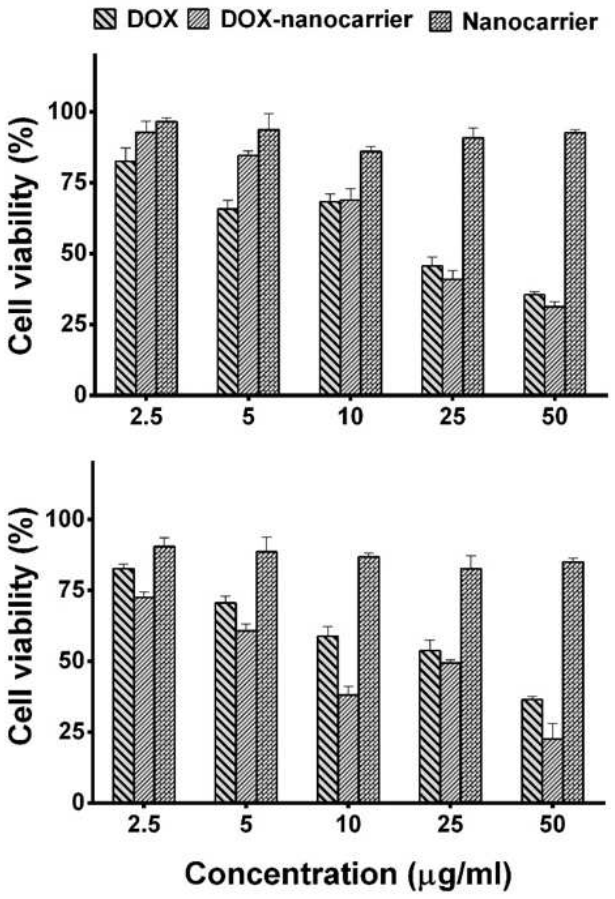

Figure 7. (a) The cytotoxicity assay measured by MTT of MCM-41-NH_2-CS-g-poly (AAm-co-AA) nanocomposite (as nanocarrier), MCM-41-NH_2-CS-g-poly (AAm-co-AA)-DOX (as DOX-nanocarrier), and free DOX on MCF7 cells after 24 h.(b) The cytotoxicity assay measured by MTT of MCM-41-NH_2-CS-g-poly (AAm-co-AA) nanocomposite (as nanocarrier), MCM-41-NH_2-CS-g-poly (AAm-co-AA)-DOX (as DOX-nanocarrier), and free DOX on MCF7 cells after 48 h.

As shown in figures 7 and 8, the viability of the cells was above 90%, and 80% respectively for the MCM-41-NH_2-CS-g-poly (AAm-co-AA) nanocomposite (as nanocarrier) at concentration 50 μg mL^{-1}. The viability of cells treated with DOX-loaded MCM-41-NH_2-CS-g-poly (AAm-co-AA) nanocomposite for 24 h is about 80% at concentration of 2.5 μg/mL. But the concentration reach to 50 μg mL^{-1}, the viability of cells treated with DOX-loaded MCM-41-NH_2-CS-g-poly (AAm-co-AA) nanocomposite significantly decrease about 30% at the same duration of incubation.

In the case of DOX-nanocarrier during 48 h, the results show that DOX-loaded MCM-41-NH_2-CS-g-poly (AAm-co-AA) nanocomposite reveal reduction in the cell viability as compare to free DOX at different concentrations. As shown the Figure 8.b, most considerable reduction in the cell viability by using DOX-loaded MCM-41-NH_2-CS-g-poly (AAm-co-AA) nanocomposite (as DOX-nanocarrier) is observed about 20% at concentration 50 μg mL^{-1}. This result confirms that DOX-loaded MCM-41-NH_2-CS-g-poly (AAm-co-AA) nanocomposite has high performance (cytotoxicity effect) in killing of cancer (MCF7) cell after 48 h incubation at concentration 50 μg/mL.

DOX is an anticancer drug. Free DOX diffuse rapidly into nucleus, and kill cancer cells by interaction with DNA. But its systemic toxicity, and quick drug degradation remain as the main problems. To solve this problem, and achieve to favorable therapeutic index, prolonged release of drug, better therapeutic results, and decreasing the side effects on the normal cells is advised the use of targeted drug delivery systems based on pH-responsive smart polymeric nanocarriers.

3.7.2. Induced apoptosis and in-vitro Cellular uptake study

In the Cells containing fragmented DNA occur Apoptosis. Apoptosis is a physiological cell death that under normal conditions, lead to remove damaged or harmful cells, and is essential for cellular homeostasis. Disorder in apoptosis leads to various diseases such as cancer, tumor resistance to drugs, etc. Some anticancer drugs such as DOX can induce apoptosis of cancerous cells by using oxidative DNA damage in the nucleus. The free DOX can enter the cancerous cells by diffusion, and interact with DNA into the nucleus. But, keeping active of free anticancer drugs after reaching at the nucleus is difficult due to the biobarriers. To overcome this problem, the nuclear targeted drug delivery systems employ to enhance anticancer drug efficiency.

To investigate the morphological change in the nucleus of an apoptosis cell use DAPI staining. Because of fluorescence feature of the 4,6-diamidino-2-phenylindol (as DAPI with blue color) is used for observation of the apoptotic cell nucleus morphology (chromatin density and fragmentation) by using fluorescence microscopy. The Figure 10 top show the DAPI staining of untreated human breast epithelial adenocarcinoma

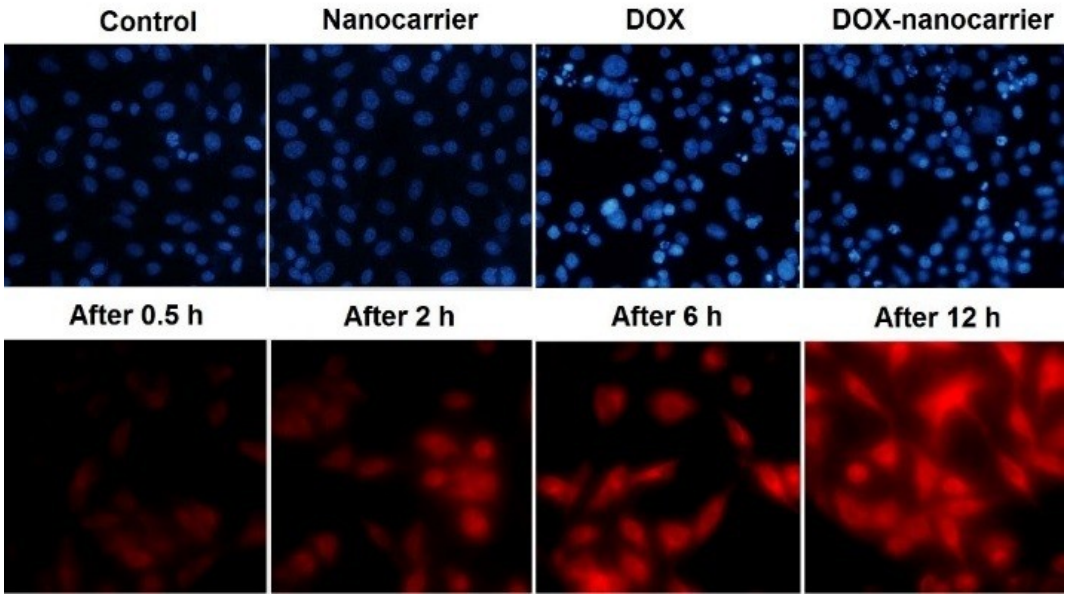

Figure 8. Fluorescence Microscopy images of untreated human breast epithelial adenocarcinoma (MCF7) cells (Control), treated MCF7 cells incubated for 2 h with MCM-41-NH_2-CS-g-poly (AAm-co-AA) nanocomposite (Nanocarrier), treated MCF7 cells incubated for 6 h with free DOX (DOX), and treated MCF7 cells incubated for 12 h with DOX-loaded MCM-41-NH_2-CS-g-poly (AAm-co-AA) nanocomposite (DOX-nanocarrier) respectively from left to right. The blue fluorescence is from 4,6-diamidino-2-phenylindole (DAPI) used to stain the nuclei, and the red fluorescence is from DOX.

(MCF-7) cells (Control), treated MCF7 cells with MCM-41-NH_2-CS-g-poly (AAm-co-AA) nanocomposite (Nanocarrier), treated MCF7 cells with free DOX (DOX), and treated MCF7 cells with DOX-loaded MCM-41-NH_2-CS-g-poly (AAm-co-AA) nanocomposite (DOX-nanocarrier) respectively from left to right. As shown in figure, no apoptotic cell was observed in the control. In the treated MCF7 cells with free DOX (DOX), were detected apoptotic cell nucleus morphology (chromatin density and fragmentation). In addition, treated MCF7 cells with DOX-loaded MCM-41-NH_2-CS-g-poly (AAm-co-AA) nanocomposite (DOX-nanocarrier) revealed higher content of apoptotic cell nucleus morphology (chromatin density and fragmentation) than free DOX.

The red fluorescence is from DOX. Due to the fluorescence feature of DOX, can used it in fluorescence microscopy studies to observe the content cellular uptake without additional marker. The Figure 10 bottom display the content cellular uptake of free DOX after incubation with MCF7 cells during 6 h, and the content cellular uptake of DOX-loaded MCM-41-NH_2-CS-g-poly (AAm-co-AA) nanocomposite (DOX-nanocarrier) after incubation with MCF7 cells during 12 h. As seen the figure, DOX-loaded MCM-41-NH_2-CS-g-poly (AAm-co-AA) nanocomposite (DOX-nanocarrier) reveal the fluorescent intensity in compare to free DOX. This observation shows clearly that DOX-loaded MCM-41-NH_2-CS-g-poly (AAm-co-AA) nanocomposite (DOX-nanocarrier) have higher capability for drug delivery to cancerous cells than free DOX. The cellular uptake mechanism of DOX-loaded MCM-41-NH_2-CS-g-poly (AAm-co-AA) nanocomposite (DOX-nanocarrier) are displayed in scheme 2.

4. Conclusions

In this research, we have fabricated polymer NCs based on (MCM-41-NH_2) nanoparticles and CS-graft-poly (AAm-co-AA) as a pH-sensitive polymer for targeted cancer therapy. The functional groups containing anionic –COOH (–COO^-), -$CONH_2$ (-$CONH^-$) charges of the polymer NCs formed hydrogen bonds with DOX (as cationic drug The release capacity of DOX from the polymer NCs as MCM-41-NH_2-CS-graft-poly (AAm-co-AA) mesoporous Si-MCM-41/polymer was measured at acidic conditions (on the human breast epithelial adenocarcinoma (MCF7) cancer cells, pH 5.3 and 40 °C). The results showed that less than 8% of loaded DOX was released from MCM-41-NH_2-CS-g-poly (AAm-co-AA)- DOX after the continuous incubation at normal physiological condition (pHs = 7.4 and 37 °C) for 75 h. while in pH 5.3 and 40 °C were nearly 90% during 75 h, indicating that the release of DOX from MCM-41-NH_2-CS-g-poly (AAm-co-AA). So, the release of DOX was as a pH-sensitive process. The cytotoxicity of the DOX loaded into MCM-41-NH_2-CS-g-poly (AAm-co-AA) on the (MCF7) cancer cells was evaluated by using MTT. result confirm that DOX-loaded MCM-41-NH_2-CS-g-poly (AAm-co-AA) has high performance (cytotoxicity effect) in killing of cancer (MCF7) cell after 48 h incubation at concentration 50 μg/mL. To investigate the morphological change in the nucleus of an apoptosis cell used DAPI staining. Treated MCF7 cells with DOX-loaded MCM-41-NH_2-CS-g-poly (AAm-co-AA) as (DOX-nanocarrier) revealed higher content of apoptotic cell nucleus morphology (chromatin density and fragmentation) than free DOX. In according with the results can be concluded that the fabricated polymer NCs as MCM-41-NH_2-

CS-graft-poly (AAm-co-AA) has high efficiency as drug delivery system for cancer therapy application.

Supporting Information Summary

(1) Experimental section: In this section we give all of experimental that we used for synthesizing of biocompatible polymer Nanocomposites based on MCM-41 nanoparticles and copolymer grafted chitosan by acrylamide and acrylic acid (CS-graft-poly (AAm-co-AA) as a pH-sensitive polymer.

Acknowledgements

Authors earnestly acknowledge the partial financial support from Payame Noor University.

Conflict of Interest

The authors declare no conflict of interest.

Keywords: Controlled drug delivery · mesoporous Si-MCM-41/ smart polymer · pH-responsive release · Cancer therapy

[1] F. Tang, L. Li, D. Chen, *Adv. Mater.* **2012**, *24*, 1504–1534.
[2] W. Feng, W. Nie, C. He, X. Zhou, L. Chen, K. Qiu, W. Wang, Z. Yin, *ACS Appl. Mater. Interfaces.* **2014**, *6*, 8447–8460.
[3] L. Pan, Q. He, J. Liu, Y. Chen, M. Ma, L. Zhang, J. Shi, *J. Am. Chem. Soc.* **2012**, *134*, 5722–5725.
[4] W. Cheng, J. Nie, L. Xu, C. Liang, Y. Peng, G. Liu, T. Wang, L. Mei, L. Huang, X. Zeng, *ACS Appl. Mater. Interfaces* **2017**, *9*, 18462–18473.
[5] Y. Zhang, C. Yen Ang, M. Li, S. Y. Tan, Q. Qu, Zh. Luo, Y. Zhao, *ACS Appl. Mater. Interfaces.* **2015**, *7*, 18179–18187.
[6] J. L. Paris, M. V. Cabanas, M. Manzano, M. Vallet-Regí, *ACS Nano.* **2015**, *9 (11)*, 11023–11033.
[7] M. Abbasian, M. M. Roudi, F. Mahmoodzadeh, M. Eskandani, M. Jaymand, *Int. J. Biol. Macromol.* **2018**, *118*, 1871–1879.
[8] A. Sepahvandi, M. Eskandari, F. Moztarzadeh, *Mater. Sci. Eng. C.* **2016**, *66*, 306–314.
[9] S. Saber-Samandari, S. Saber-Samandari, *Mater. Sci. Eng. C.* **2017**, *75*, 721–732.
[10] A. Hakeem, R. Duan, F. Zahid, Ch. Dong, B. Wang, F. Hong, X. Ou, Y. Jia, Xiaoding Lou, F. Xia, *Chem. Commun.* **2014**, *50*, 13268–13271.
[11] Z. Shariatinia, Z. Zahraee, *J. Colloid Interface Sci.* **2017**, *501*, 60–76.
[12] A. Pourjavadi, Z. Mazaheri Tehrani, S. Jokar, *Polymer (Guildf).* **2015**, *76*, 52–61.
[13] A. Abbaszad Rafi, M. Mahkam, S. Davaran, H. Hamishehkar, *Eur. J. Pharm. Sci.* **2016**, *93*, 64–73.
[14] M. Ghorbani, F. Mahmoodzadeh, B. Jannat, N. Fathi Maroufi, B. Hashemi, L. Roshangar, *Polym. Adv. Technol.* **2019**, *30*, 1847–1855.
[15] Q. Yang, S. Wang, P. Fan, L. Wang, Y. Di, K. Lin, F. S. Xiao, *Chem. Mater.* **2005**, *17*, 5999–6003.
[16] M. Abbasian, M. Judi, F. Mahmoodzadeh, M. Jaymand, *Polym. Adv. Technol.* **2018**, *29*, 3097–3105.
[17] S. Angelos, Y. W. Yang, K. Patel, J. F. Stoddart, J. I. Zink, *Angew. Chem. Int. Ed.* **2008**, *47*, 2222–2226; *Angew. Chem.* **2008**, *120*, 2254–2258.
[18] A. Bernardos, E. Aznar, M. D. Marcos, R. M. Máñez, F. Sancenón, J. Soto, J. M. Barat, P. Amorós, *Angew. Chem. Int. Ed.* **2009**, *48*, 5884–5887; *Angew. Chem.* **2009**, *121*, 5998–6001.
[19] A. Popat, B. P. Ross, J. Liu, S. Jambhrunkar, F. Kleitz, S. Z. Qiao, *Angew. Chem. Int. Ed.* **2012**, *51*, 12486–12489; *Angew. Chem.* **2012**, *124*, 12654–12657.
[20] K. Patel, S. Angelos, W. R. Dichtel, A. Coskun, Y. W. Yang, J. I. Zink, J. F. Stoddart, *J. Am. Chem. Soc.* **2008**, *130*, 2382–2383.
[21] P. Wang, Sh. Chen, Z. Cao, G. Wang, *ACS Appl. Mater. Interfaces.* **2017**, *9*, 29055–29062.
[22] H. Kobayashi, B. Turkbey, R. Watanabe, P. L. Choyke, *American Chemical Society* **2014**, 2093–2100.
[23] J. Liu, C. Detrembleur, M. C. D. Pauw-Gillet, S. Mornet, L. Vander Elst, S. Laurent, Ch. Jérôme, E. Duguet, *J. Mater. Chem. B* **2014**, *2*, 59–70.
[24] J. Liu, J. Bu, W. Bu, Sh. Zhang, L. Pan, W. Fan, F. Chen, L. Zhou, W. Peng, K. Zhao, J. Du, J. Shi, *Angew. Chem. Int. Ed.* **2014**, *53*, 4551–4555; *Angew. Chem.* **2014**, *126*, 4639–4643.
[25] F. Mahmoodzadeh, M. Hosseinzadeh, B. Jannat, M. Ghorbani, *Polym. Adv. Technol.* **2019**, *30*, 1344–1355.
[26] H. Batmani, N. Noroozi Pesyan, F. Havasi, *Microporous Mesoporous Mater.* **2018**, *257*, 27–34.
[27] F. Mahmoodzadeh, B. Jannat, M. Ghorbani, *Int. J. Biol. Macromol.* **2019**, *126*, 517–524.

Submitted: May 20, 2020
Accepted: September 24, 2020